Japanese Journal of Applied Physics
Vol. 28, No. 10, October, 1989, pp. [illegible]-2064

Multi-Beam Concepts for Nanometer Devices

B. Lischke, W. Bennecke††, M. Brunner,
K. H. Herrmann†, A. Heuberger††, E. Knapek,
P. Schäffer† and U. Schnakenberg††

Siemens AG, Forschung für Materialwissenschaften und Elektronik, 8000 München 83, FRG
†Institut für Angewandte Physik, Universität Tübingen, 7400 Tübingen, FRG
††Institut für Mikrostrukturtechnik der FhG, 1000 Berlin, FRG

(Received July 5, 1989; accepted for publication August 19, 1989)

To overcome the throughput limitations in electron beam nanolithography, a multi beam system is proposed. Theoretical considerations show that this e-beam comb-probe printer with 1024 probes will be capable of combining 25 nm resolution with a maximum beam current of 5 μA. This allows an exposure speed of 0.1 cm²/s, which is orders of magnitude superior to today's most advanced equipment. In addition, the multi beam principle is considered for nanometer pattern inspection and for ion-beam techniques. The basic concepts for these applications are presented. Practical feasibility investigations are the subject of current research.

KEYWORDS: Electron beam lithography, nanometer pattern, multi beam concept, comb probe printer, X-ray mask making, Wafer exposure, multi beam inspection, multi ion beam techniques

§1. Introduction

There are several main areas of application for e-beam lithography. Two of them are a) mask making for all kinds of optical lithography,[1-5] X-ray proximity printing[6] and ion beam steppers[7-9] and b) direct wafer exposure for the development of new devices with extremely small lateral dimensions such as new cell concepts for silicon technology,[10] GaAs electronics,[11] optoelectronic components or quantum devices.[12] For research and fabrication of these ultra small devices, the throughput of today's conventional e-beam nanolithography equipment is orders of magnitude smaller than that required. In this paper we would like to discuss e-beam nanolithography with special focus on the throughput problem and propose a multi beam (MB) system for obtaining throughput improvements.[13] This comb probe concept will be applied to the inspection of nanometer patterns and finally some novel multi ion beam techniques and their applications will be presented.

§2. Throughput in E-Beam Nanolithography

When extremely small patterns below 500 nm have to be exposed, throughput is an ongoing problem. For one 6-inch wafer with 50% coverage and a 20 μC resist for example, the exposure time in a conventional e-beam pattern generator with 10 nm spot and 50 A/cm² current density amounts to 1 year per level! Thus the overhead in a lithography system such as loading, beam alignment, stage movement a.s.o. is of minor importance and the exposure time becomes the determining quantity. In the case of exposure-limited throughput T_{expo} we obtain (see Fig. 1)

$$T_{expo} \leq \frac{1}{X}\frac{i}{C} = \frac{1}{X}\frac{j}{C} mn\delta^2 \left[\frac{\mathrm{cm}^2}{s}\right], \qquad (1)$$

which is determined by the beam current density j (beam current i), the coverage X, the resist sensitivity C, and the average number $m \cdot n$ of the smallest exposure elements δ^2 exposed in parallel. The smallest exposure element δ^2 is determined by the smallest possible spot size diameter δ in a round-beam system (half width of the intensity distribution) or the edge slope δ in a variable-shaped spot system (resolution). To expose an element δ^2, a minimum number of electrons N is necessary. N has to be sufficiently large to keep the statistical fluctuations below a desired level. The smallest surface charge density (resist sensitivity) is then

$$C \geq \frac{Ne}{\delta^2}. \qquad (2)$$

For a pattern element of 100 nm diameter exposed with about 10000 electrons,[14] eq. (2) yields 16 μCoulomb·cm⁻² when keeping the dose fluctuations by shot noise below 1%. Combining eqs. (1) and (2) and taking into account that the critical demension d_c is correlated with the resolution δ of the system $d_c = m\delta$ ($m = 4 \ldots 5$), we obtain the relationship

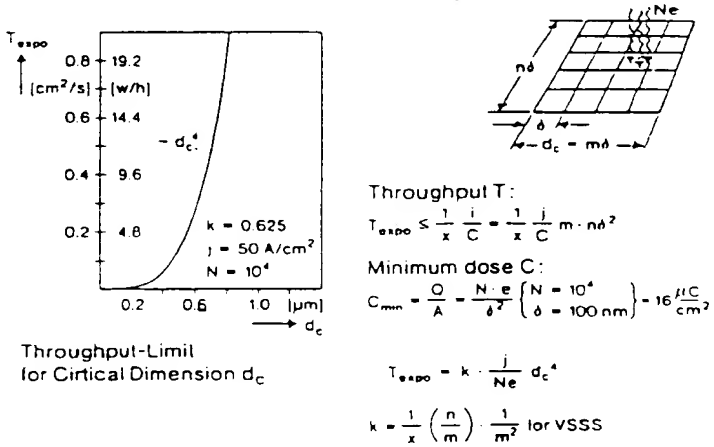

Fig. 1. Limits of exposure speed for single spot systems.

$$T_{expo} = \frac{1}{\chi}\left(\frac{n}{m}\right)\cdot\frac{1}{m^2}\frac{j}{Ne}\cdot d_c^4 \qquad (3)$$

which is plotted in Fig. 1 for the parameters indicated. (In reality, the throughput dependence T_{expo} on the critical demension d_c is more complicated, but we will restrict ourselves to these approximations for simplicity). The result indicates (eq. 3), that the throughput T_{expo} decreases by more than 3 orders of magnitude when going from a 0.6 μm to a 0.1 μm pattern, due to the statistical nature (shot noise) of electron beams and the fact that smaller beams contain less current.

2.1 *The multi-beam concept*

Conventional writing systems with a single spot[15] expose one image point at a time, which is a flexible method but leads to low throughput. E-beam steppers in contrast, provide a maximum exposure speed[16,17] but no pattern flexibility at all. The basic idea behind the multi-beam (MB) concept is to combine the flexibility of a writing system with the speed of an e-beam stepper, leading to the principle of a comb probe printer.

Figure 2 represents a schematic of one possible configuration of the printer. A ribbon beam illuminates a linear array of square holes in a thin membrane aperture plate to form shaped beams. Each beamlet is provided with its own microcapacitor (deflection plate) allowing probe deflection for individual beam blanking (see side view of Fig. 2). The pattern is generated by stepping the complete comb probe sideways to fill in the gaps between the probes and moving the stage normal to the comb probe. Imaging and raster-scan defelection of all beams (several hundreds up to thousands are possible) is effected collectively. However, intensity modulation is applied to each beam individually, similarly to a method reported earlier.[18,19]

First experiments indicate that it seams feasible to form hundreds or even thousands of deflection elements, thus meeting the requirements of the printing system. The goal for such a system is to combine nm resolution with a beam current of a few μA on the wafer target. This should result in an exposure speed of about 0.1 cm^2/s for patterns with 100 nm lines, which is several orders of magnitude larger than that of today's conventional equipment.

The beam current on the wafer can be further improved by feeding each electron beamlet by its own source. New types of photoelectron[20] or solid-state[21-23] emitters seem quite promising for this purpose. The sources are projected into the plane with the control plate or the latter is substituted by the source configuration itself, which is shown in Fig. 3. Each source consists of a p-n diode, biased in an avalanche breakdown. Electrons diffusing into the strong field within the p-n region are accelerated directly into the vacuum. Because of the small capacitance of the sources (source diameter about 1 μm) they can be switched on and off very fast (up to the GHz range) and their brightness is comparable to field emitters. Thus a great deal of further improvement capacity is available within the MB (comb probe) principle, and stage speed and data transfer rate will become the dominant factors that limit throughput in nanolithography.

2.2 *Requirements for multi-beam systems*

One of the most stringent requirements in nanolithography is the placement accuracy of the pattern. The principle of the comb probe printer is especially adapted to this problem. Because of the small deflection of the comb probe (deflection amplitude $< 1\ \mu$m) all nonlinearities due to deflection distortion and beam settling are avoided. (Modern metrology tools for nanometer pattern measurement use the same principle: fixed beam, moving specimen). In addition, the blanking elements are positioned in the object plane and thus do not cause pattern displacement by beam defelction. For these reasons, the comb-probe principle seems to be well suited to nanolithography pattern generators.

To guarantee full flexibility of a MB system, the electron probes have to be as small as the underlying CAD pattern grid (nm range). This is different in size for reticle making and direct wafer exposure. To allow for both applications in the same instrument, we introduce the concept of a variable shaped multi beam (VSMB), depicted in Fig. 4. Instead of one aperture plate, two of them are employed for MB-formation. For mask making they coincide; for high resolution direct wafer exposure one

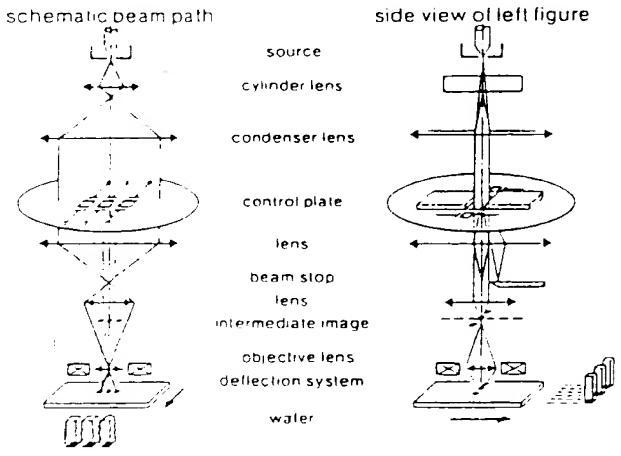

Fig. 2 Principle of a multi-beam system (e-beam comb probe printer). The line printer system generates patterns with a large number of electron probes that are blanked individually. The line printing ferquency in the MHz-range corresponds to GHz pixel frequency.

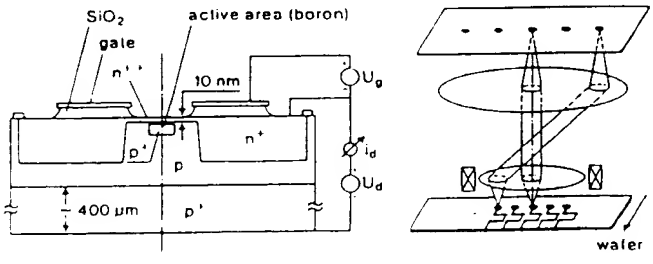

Fig. 3 Comb-probe printer principle with multi-beam solid states emitters. Each electron probe is fed by its own source for further probe current improvement. Beam blanking is performed by switching the emitters on and off. (van Gorkom and Hoeberechts, 1986)

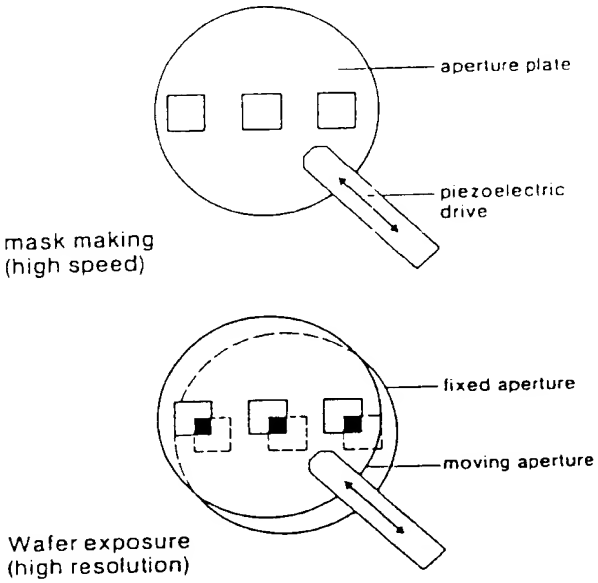

Fig. 4. With the variably shaped multi-beams (VSMB) different requirements for reticle making and direct wafer exposure can be met. Probe shaping is performed by moving one aperture plate with respect to a fixed one.

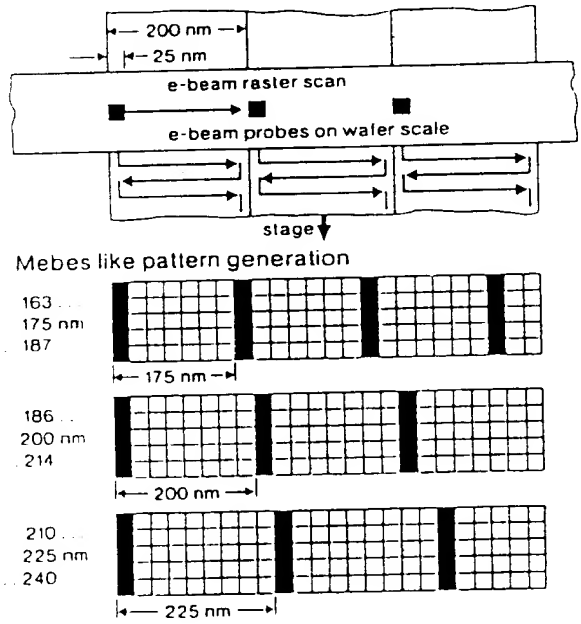

Fig. 5. Matching the comb probe to arbitrary grids by combining a small demagnification change (7%) with a suitable blanking sequence.

aperture is shifted by means of a piezoelectric drive, resulting in smaller probes but less current. Thus the probe size can be easily adapted to the desired pattern.

In multi-beam approaches, the probe can only be deflected by a collective procedure.[24] Therefore it is difficult to vary the relative position of individual beams, although this is necessary to take design grid variations into account.

This problem will be solved for the e-beam printer by making provision for a demagnification change of several percent together with a small rotation of the complete comb probe. How to fit the pitch of the comb probe to a given design grid is best explained by using the numerical example in Fig. 5. The complete comb probe with a pitch of 200 nm is projected onto the wafer and scanned in a Mebes-like raster while the stage is moving normal to the comb probe (Fig. 5 upper part). By using a suitable blanking sequence, a pitch of 175 nm can be realized. Combining this pitch with a $\pm 7\%$ magnification change allows a range from 163 to 187 nm for the pitch to be covered. The other examples in Fig. 5 relating to 200 nm and 225 nm pitch clearly demonstrate the procedure for obtaining arbitrary grid patterning. The problem imposed on the electron optics is to maintain full aberration compensation when changing the magnification. The method described, however, should be sufficient to fit the pitch of the comb probe to arbitrary design grids. Accurate control of pattern dimensions requires the proximity effect[25] to be corrected for. This is possible by suitably adapting the exposure dose. The largest dose determines the stepping frequency of the comb probe: a smaller dose per image element can be achieved by using shorter blanking periods.

2.3 *Instrument design*

A schematic of one possible MB configuration is shown in Fig. 6. The ribbon-beam illumination should provide a current density $\geq 50\ A/cm^2$ in the wafer plane. A line-shaped cathode is magnified by a telecentric condenser lens system for the illumination of the 20 mm long array of 1024 square holes. A magnetic multipole inside condenser 2 compensates both the spherical aberration and the astigmatism. The electron probes are demagnified and imaged onto the wafer by a double

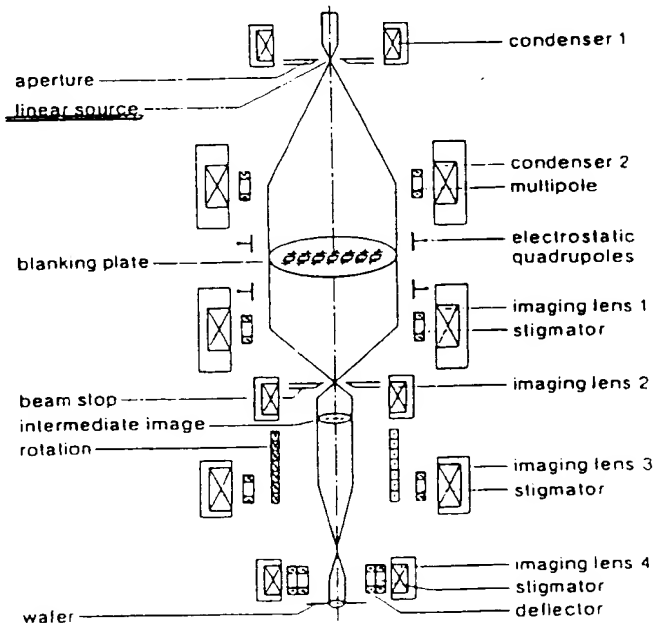

Fig. 6. Schematic of an instrument design.

telecentric imaging system. This has to resolve 10,000 lines per field without dynamic corrections. It generates a printing track of 200 μm width with 20 nm resolution (minimum probe size). The proper magnification is set by the lens excitations and the rotation of the comb probe is aligned with respect to the stage by a weakly excited coil. Fast magnification and rotation change are performed by electrostatic multipoles if necessary. The distortion of the comb probe must be completely corrected by means of lens excitations and the pole piece shape.[16] Preliminary calculations yield aberration discs of about 30 nm resolution across an image field diameter of 200 μm (Fig. 7).

The most critical part of the system is the control plate shown in Fig. 8, consisting of the probe-forming aperture plate and the deflection plate for individual beam blanking. The aperture plate is realized with electroplating a thin Au-membrane or with a 3 μm thick silicon foil using standard micromechanical technology. The fabrication of the deflection plate is illustrated in Fig. 9. Starting from a 4-inch (100)-orientated wafer, it is covered with a low pressure CVD-Si_3N_4 layer for passivation. After etching, a Cr/Au metallization is applied as a plating base, followed by lithography and Au-electroplating to form the interconnection lines. The microcapacitors are electroplated in resist up to a thickness of approximately 25 μm. The blanking plate is finished by anisotropic wet etching of the silicon bulk material from the rear side and by removing the plating base.

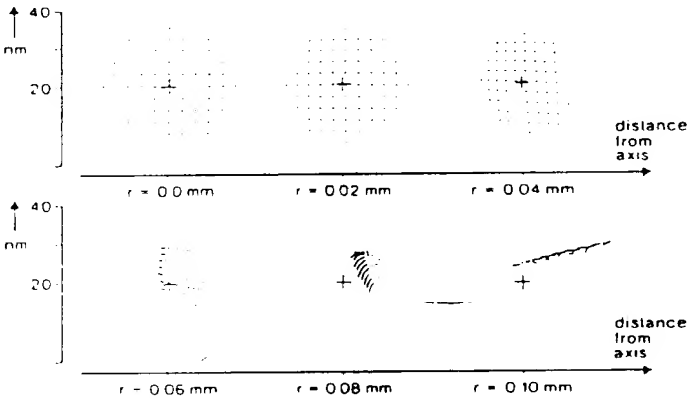

Fig. 7. Calculated aberration discs indicating 30 nm resolution within 200 μm field size. Upper: close to axis, Lower: off axis.

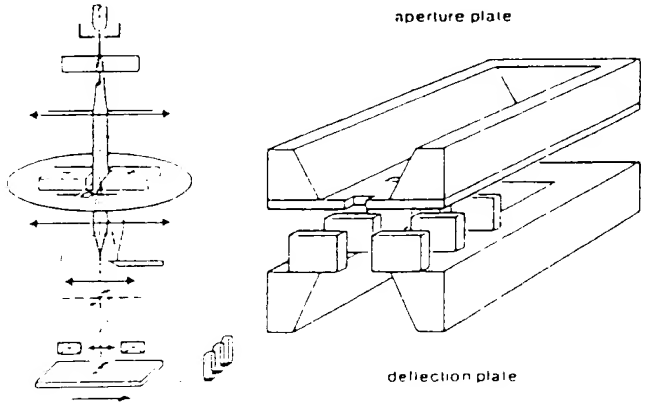

Fig. 8. Control plate, consisting of a probe forming aperture plate and a deflection plate for individual beam blanking.

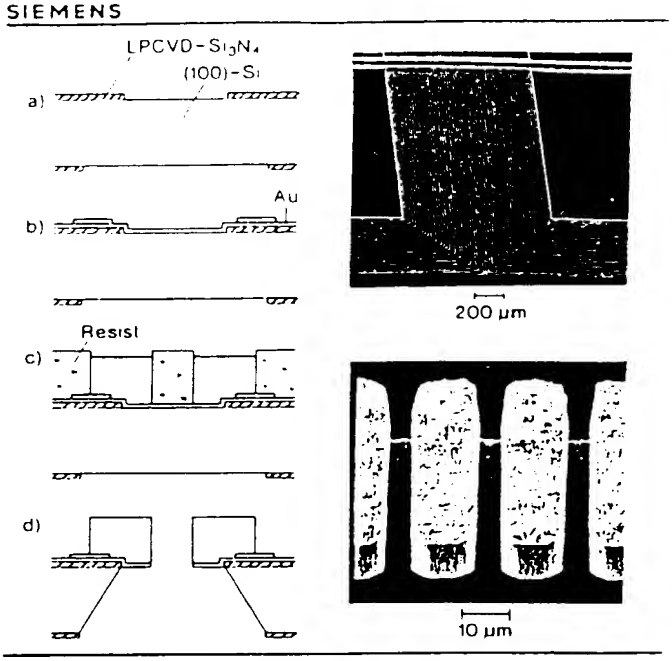

Fig. 9. Fabrication of deflection plate (left) and microcapacitors with interconnection lines (right).

Special software and electronic hardware is required to control the e-beam comb probe and to supply the capacitors with the deflection voltages respectively. Although the line-printing frequency is relatively low (several MHz), the complete pattern information for the full line has to be applied simultaneously to all electron probes.

At present, a special pattern generator is being realized to control 64 out of 1024 microcapacitors in parallel with a clock cycle time of several MHz.

2.4 *Throughput comparison of multi-beam (MB) versus variable shaped spot (VSS) systems*

In accordance with eq. (1), the exposure-limited throughput for MB-systems is proportional to $\overline{M}$, the average number of usable beamlets for a pattern, where $\overline{m \cdot n}$ is the average number of exposure elements in VSS systems.[26-29] If we assume the same current density on the target for both systems, we simply get

$$\frac{T_{MB}}{T_{VSS}} = \frac{\overline{M}}{\overline{mn}} \tag{4}$$

As long as this ratio is > 1, the MB throughput is superior to that of VSS due to the larger number of exposure elements printed at a time. Figure 10 illustrates

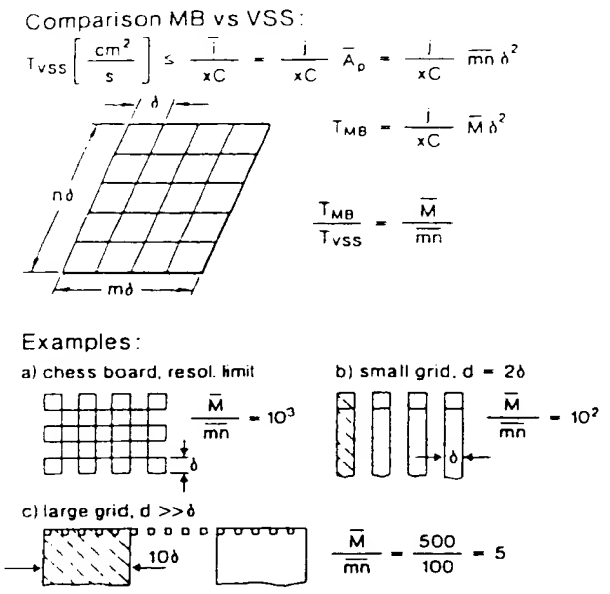

Fig. 10. Comparison of exposure time limited throughput T; multi-beam (MB) versus variably shaped spot (VSS) for three different examples. The mean value of the beam current $\bar{i}$ is expressed by the current density j and the mean value of the probe cross section $\bar{A}_p$. An e-beam system is suprior to others, that allows an optimum number of exposure elements $\overline{m \cdot n}$ (or $\bar{M}$) to be exposed in parallel.

three examples having 50% coverage, going from a high resolution chessboard pattern to grids with a coarse pitch. The anlalysis demonstrates that MB yields ultimate throughput for high resolution nanolithography (pattern close to the resolution limit, bent or tilted lines, small grids etc.), while VSS is superior in the case of coarser structures and low coverage. (In the examples indicated we assumed the maximum aspect ratio of VSS to be 1:10 and the largest cross section of the variable shaped spot 100 δ^2, δ being the resolution of the system). In the comparison between MB and VSS it should be added that the MB system seems to have advantages with respect to resist heating. The comb probe extends over a line of 200 μm, which is large compared with the sattering range of electrons of a few micron, so that adiabatic heating is less severe.

§3. Multi-Beam Nanometer Pattern Inspection

When evaluating the physics of defect inspection of nanometer patterns with electron beams, the throughput problem arises from the statistical nature of electrons. Keeping the fluctuations of electrons (shot noise) small compared with the defect signal amplitude, this leads to an inspection throughput < 1 cm^2/h for 100 nm patterns inspected with conventional systems.[30]

In order to improve the throughput, an e-beam technique utilizing the multi-beam concept is proposed. It uses several beams in parallel to scan across the sample, each beam generating secondary electrons (Fig. 11). (Only the beam of primary electrons PE is drawn in Fig. 11, but several sources and the corresponding probes on the mask/wafer are indicated). Each of these primary beams is thus equivalent to the beam in a scanning electron

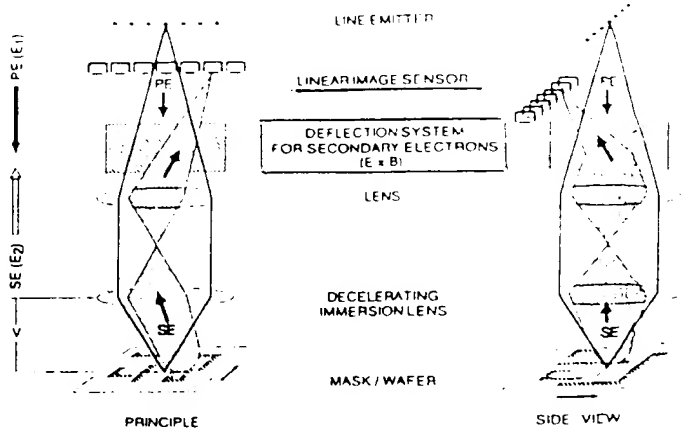

Fig. 11. Multi-beam inspection of nanometer patterns with parallel detection of secondary electrons.

microscope. The comb of beams is focused onto the sample using a decelerating immersion lens with a voltage V between sample and pole piece. This voltage in turn accelerates the secondary electrons SE which are generated by each probe in the opposite direction. A magnified image of the illuminated elements is thus formed in the upper part of the electron-optical column. (Again only one of several SE paths is drawn in Fig. 11). This subfunction of the system is equivalent to an emission electron microscope. A deflection system, *e.g.* a Wien filter, is used to place the secondary-electron image off axis onto a linear image sensor.

This detector provides sensitive areas, each of which detects the secondary electrons generated by its corresponding primary probe. The signals generated by the different primary beams are thus separated from each other. A parallel interface to a computer is necessary to evaluate the accumulated information in real time while the comb probe is scanning. The conditions for imaging the demagnified comb source onto the sample and simultaneously imaging the magnified source of secondary electrons onto the linear image sensor can be met by allowing intermediate images in the secondary electron ray path and by adjusting the energies E_1 and E_2 (Fig. 11). These values can be tuned by the primary beam voltage and by the voltage on the immersion lens. The resulting throughput improvement is proportional to the number of primary beams and research work is under way for its experimental verification.

§4. Multi Ion-Beam Techniques

The scattering properties of ions in comparison with electrons are best explained by the Monte Carlo calculations of Karapiperis[31] and Kyser,[32] depicted in Fig. 12. Ions with an energy of 60 keV penetrating a silicon substrate covered with PMMA-resist are decelerated in a small volume, so that the locally deposited energy density is quite high. Electrons on the other hand are scattered in a larger volume, leading to the proximity effect.[25] From these scattering properties, ions seem quite promising for nanolithography without suffering from the proximity

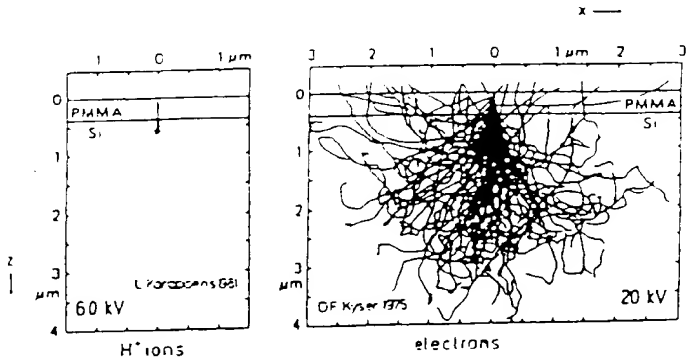

Fig. 12. Scattering properties of ions in comparison with electrons (L. Karapiperis *et al*, 1981; D. F. Kyser *et al*, 1975).

effect. For focused ion beam lithography the same throughput problem exists as for electrons. Therefore the question may be raised as to whether the MB-concept can be transferred to ions. In addition, it would be helpful for focused ion-beam milling (*e.g.* mask repair) in order to avoid redeposition and to improve speed.

The deflection angle α of charged particles in a homogeneous electric field (capacitor) is given by (see Fig. 13)

$$\alpha = \frac{l}{2d}\frac{U}{U_0} \tag{5}$$

(l = capacitor length, d = capacitor spacing),

which is obviously independent of the particle mass. Thus the same deflection device can be used for ions as well as electrons. The blanking frequency, however, is influenced by the large ion mass causing a low drift velocity through the deflector. The ultimate blanking frequency

$$f = \frac{1}{T} = \frac{1}{2\Delta t} \text{ with } \Delta t = \frac{l}{v} \tag{6}$$

is obtained by $v = (2qU_0/m)^{1/2}$ and eq. (5):

$$f = \frac{1}{4}\frac{U}{\alpha d}\left(\frac{2q}{mU_0}\right)^{1/2} \tag{7}$$

A fixed deflection angle α, a capacitor voltage U and a specific ion energy $q \cdot U_0$ require the distance between the blanking plates d to be extremely small to compensate for the large ion mass m. The control plate as discussed in §2.3 exactly meets these requirements and may thus be used in an ion-optical arrangement.

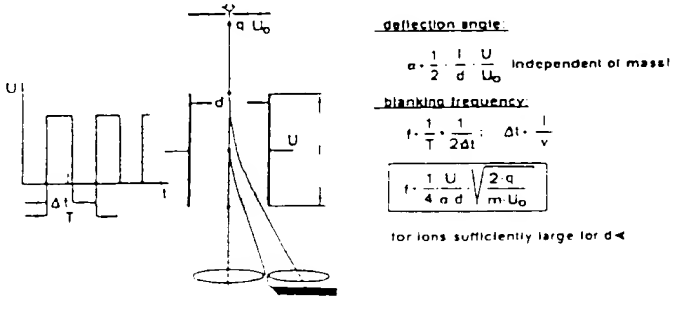

Fig. 13. Deflection angle and blanking frequency for charged particles. High speed beam blanking for ions is obtained by a small capacitor plate distance d. The control plate meets this requirement.

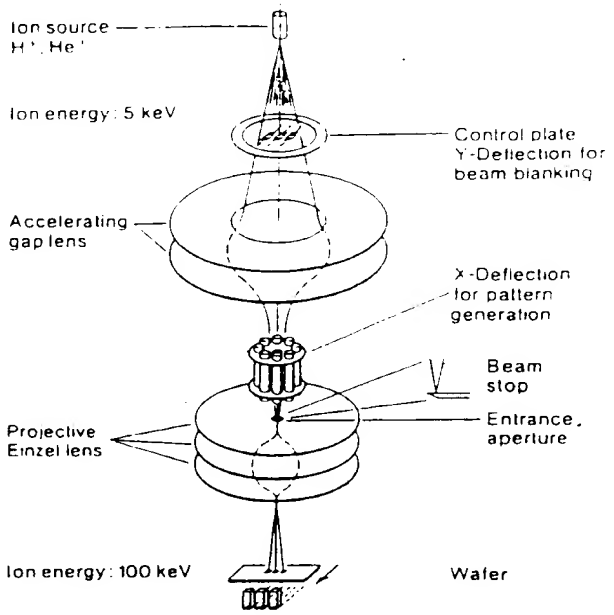

Fig. 14. Ion beam stepper with modifications (control plate, ribbon beam illumination, beam stop) for multi beam applications (by permission of IMS, Vienna, Austria).

The ion beam stepper seems to be best suited to introduce the MB-concept into ion optics,[7,33] but with two modifications as shown in Fig. 14. The mask has been replaced by a control plate for generating a number of individual ion probes. It is illuminated by an ion ribbon-beam to improve exposure efficiency. Minideflection of the resulting comb probe is performed by means of an electrostatic multipole. Focusing and alignment are performed by standard procedures.

§5. Summary

In summary, we introduced the multi-beam concept for applications in nanolithography, in pattern inspection, and in ion-beam techniques. Using this principle, it seems feasible to improve throughput by orders of magnitude compared with today's most advanced equipment.

Acknowledgements

This work was partly funded by the German government (BMFT Project No. NT 2727); the authors alone are responsible for the content

References

1) N. C. Yew: Industrial Research (Sept. 1976) 92.
2) R. A. Geshner: Solid State Technol. 22 (1979) No. 6, 69.
3) M. H. Shearer, H. Takumura, M. Isobe, N. Goto, K. Tanaka and S. Miyauchi: J. Vac. Sci. & Technol. B4 (1986) 64
4) H. C. Pfeiffer: Opt. Eng. 26 (1987) 325.
5) S. Hamaguchi, J. Kai and H. Yasuda: J. Vac. Sci. & Technol. B6 (1988) 204.
6) A. Heuberger: J. Vac. Sci. & Technol. B6 (1988) 107.
7) G. Stengl, H. Loschner and J. Muray: *18th Int. Conf. on Solid*

State Devices and Materials, Tokyo, 1986 (Business Center for Academic Societies Japan, Tokyo, 1986) p. 29.

8) R. Fischer, E. Hammel, H. Loscher, A. Stengl, P. Wolf, H. Kraus and G. Stangl: Microcircuit Eng. (Int. Conf. on Microlithography), Interlaken, Switzerland (Sept. 1986) 193.
9) P. Miller: Proc. SPIE 1089 (1989) 26.
10) G. A. Sai-Halasz: ESSDERC, 17th European Solid State Device Research Conference (1987) 71.
11) TRW Electronic Systems Group, ASM Newsletter (Sept. 1987) 1.
12) J. N. Randall and M. A. Reed: 33rd Int. Symposium on Electron, Ion and Photon Beams, Monterey, CA (May 1989), to be published in J. Vac. Sci. & Technol. B7 (1989).
13) B. Lischke, G. Christaller, K. H. Herrmann, A. Heuberger, E. Knapek, H. Kniepkamp, H. Rose, W. Ruttenauer and G. Siegel: Microcircuit Eng. (Int. Conf. on Microlithography), Vienna, Austria (Sept. 1988) 199.
14) Y. Iida: *17th Conf. on Solid State Devices and Materials, Tokyo, 1985* (Business Center for Academic Societies Japan, Tokyo, 1985) p. 357.
15) M. J. Verheijen and L. A. Fontijn: Microcircuit Eng. (Int. Conf. on Microlithography), Vienna, Austria (Sept. 1988) 419.
16) B. Lischke and W. Münchmeyer: Optik 50 (1978) 315.
17) B. Lischke, J. Frosien, K. Anger and W. Münchmeyer: Optik 54 (1979) 325.
18) H. C. Pfeiffer: IEEE Trans. Electron Devices, ED-26 (1979) 663.
19) M. G. R. Thomson, R. J. Collier and D. R. Herriott: J. Vac. Sci. & Technol. 15 (1978) 891.
20) P. May, J. M. [illegible]eat and G. Chin: Appl. Phys. Lett. 51 (1987) 145.
21) G. G. P. van Gorkom and A. M. E. Hoeberechts: J. Vac. Sci. & Technol. B4 (1986) 108.
22) A. M. E. Hoeberechts and G. G. P. van Gorkom: J. Vac. Sci. & Technol. B4 (1986) 105.
23) G. G. P. van Gorkom and A. M. E. Hoeberechts: J. Vac. Sci. & Technol. A5 (1987) 1544.
24) I. Brodie, E. Westerberg, D. Cone, J. Muray, N. Williams and L. Gasiorek: IEEE Trans. Electron Devices, ED-28 (1981) 1422.
25) S. A. Rishton and D. P. Kern: J. Vac. Sci. & Technol. B5 (1987) 135.
26) E. Goto, T. Soma and M. Idesawa: J. Vac. Sci. & Technol. 15 (1978) 883.
27) J. Trotel: J. Vac. Sci. & Technol., 15 (1978) 872.
28) M. G. R. Thomson, R. J. Collier and D. R. Herriott: J. Vac. Sci. & Technol. 15 (1978) 891.
29) H. C. Pfeiffer: J. Vac. Sci. & Technol. 15 (1978) 887.
30) F. E. Endruschat, M. Börner and K. H. Müller: Microcircuit Eng. (Int. Conf. on Microlithography), Vienna, Austria (Sept. 1988) 401.
31) L. Karapiperis, J. Adesida, C. A. Lee and E. D. Wolf: J. Vac. Sci. & Technol. 19 (1981) 1259.
32) D. F. Kyser and N. S. Viswanathan: J. Vac. Sci. & Technol. 12 (1975) 1305.
33) F. Paschke: Mikroelektronik 3 (H2) (1989) 56.